Copy 6
RM L55F20

NACA RM L55F20

NACA

RESEARCH MEMORANDUM

HYDRODYNAMIC PRESSURE DISTRIBUTION OBTAINED WITH A STREAMLINE BODY EQUIPPED WITH CHINE STRIPS

By Bernard Weinflash

Langley Aeronautical Laboratory
Langley Field, Va.

CLASSIFICATION CHANGED

To UNCLASSIFIED

By authority of NACA Res abs FRN-116 effective Date June 20, 1957
al 7-8-57

NATIONAL ADVISORY COMMITTEE
FOR AERONAUTICS

WASHINGTON
September 1, 1955

NACA RM L55F20

NATIONAL ADVISORY COMMITTEE FOR AERONAUTICS

RESEARCH MEMORANDUM

HYDRODYNAMIC PRESSURE DISTRIBUTION OBTAINED WITH A STREAMLINE BODY EQUIPPED WITH CHINE STRIPS

By Bernard Weinflash

SUMMARY

A limited investigation was made to determine the nature of the pressure distribution and the order of magnitude of the pressures on a streamline body moving on a water surface. The body of revolution was equipped with chine strips and had a fineness ratio of 9. Pressures were measured at selected values of speed, trim, and wetted length. These parameters were selected to obtain pressures in regions where negative forces were indicated by force data previously obtained and to obtain some effects of individual parameters.

The results from this investigation indicate that there is a characteristic pattern of hydrodynamic pressure distribution for streamline bodies equipped with chine strips and moving on a water surface. In a longitudinal direction moving aft, the pressure rises to a positive peak at the stagnation line, then decreases usually to a negative value and finally increases to a small positive value. In a transverse direction from the lower profile line, the positive pressures generally decreased at first and then increased to a peak just inboard of the chine strips. Negative pressures generally decreased transversely from the profile line without a pronounced peak at the chine strip. The maximum negative pressure measured was about 0.25 pound per square inch.

INTRODUCTION

Hydrodynamic force tests of reference 1 on models of streamline bodies modified by narrow chine strips have indicated that such forms may be suitable for hulls of water-based airplanes. They are of particular interest when used in conjunction with hydro-skis or hydrofoils. Streamline bodies are also of hydrodynamic interest for use as wing-tip floats and as containers for external stores. However, the presence of negative pressures was detected during the force tests of these streamline bodies. Knowledge of the magnitude and distribution of these pressures and of the

[redacted]

pressure distribution in general is essential to an understanding of the forces acting on such bodies.

Accordingly, this paper gives the results of an investigation made with a streamline body to obtain hydrodynamic pressure distributions for a few selected test conditions expected to be of most interest based on the findings of the investigation reported in reference 1. The model tested had the same dimensions as the fineness-ratio-9 model used in the force tests reported in reference 1.

SYMBOLS

C_{V_Q}	speed coefficient based on hull volume, $\dfrac{V}{\sqrt{gQ^{1/3}}} = 0.211V$
d	diameter of model, in.
l	wetted length, in.
L	overall length of model, 46.75 in.
p	measured dynamic pressure on model (does not include static displacement), lb/sq in.
q	dynamic pressure at stagnation point, $\dfrac{(\rho/2)V^2}{144}$, lb/sq in.
Q	volume of hull, 0.338 cu ft
V	speed, fps
x	station measured from nose of model along center line, in.
θ	central angle measured outboard from lower profile line, deg
λ	linear distance measured along center line from rear of model, in.
λp	value of λ for maximum positive pressure on lower profile line, in.
ρ	mass density of towing-tank water, 1.97 slugs/cu ft
τ	trim, angle between center line of model and horizontal, deg

DESCRIPTION OF MODEL

The model was a body of revolution defined by the offsets given in table I. A photograph of the model is shown in figure 1 and some construction details are shown in figure 2. The model was constructed by forming a clear plastic shell parted into two halves along a horizontal plane of symmetry and assembling the two halves around a brass frame. Narrow full-length chine strips were located on the lower half of the model along the lines of intersection formed by passing planes through the model center line at an angle of 45° from the vertical as indicated in figure 2.

There were 246, 0.024-inch-diameter orifices located on the bottom of the model in five longitudinal rows defined by passing planes through the center line of the model at angles of 0°, 15°, 30°, 45°, and 60° to port of the lower profile line. The 45° line of orifices was placed just inboard of the chine strip. The spacing and location of the orifices along these profile lines are given in table II. The orifices were drilled perpendicular to the surface of the plastic hull and special care was taken to insure clean sharp edges. This was in accordance with the findings of references 2 and 3 where it was shown that such precautions are necessary to make accurate pressure measurements. Stainless-steel tubes of 0.0625-inch inside diameter were inserted in the model at each orifice location as shown in figure 2 to produce a connection for the flexible plastic tubing leading to the manometer.

APPARATUS AND PROCEDURE

Tests were made with the small model towing gear of Langley tank no. 2. The model was towed at fixed speeds, trims, and drafts. The conditions tested are given in the following schedule:

Run	Speed, V, fps	C_{V_Q}	Trim, τ, deg	Wetted-length ratio, l/L	Chine strips
1	30	6.33	4	0.58	On
2	50	10.55	4	.58	On
3	65	13.72	4	.58	On
4	30	6.33	8	.58	On
5	30	6.33	4	.83	On
6	20	4.22	4	.79	On
7	20	4.22	4	.79	Off

Runs 1 and 7 were selected because the force test data of reference 1 indicated large negative forces acting under these conditions. Runs 2 to 6 were selected to give the widest variation possible in the parameters being compared within the scope of the force tests of reference 1.

The method of measuring the pressure is shown schematically in figure 3 and was developed for the tests reported in reference 3. The pressures were transmitted from the model orifices to the mercury manometer tubes by fresh water. In order to prevent the positive pressures on the model from forcing the salt water of the towing tank into the system as the towing carriage was brought up to speed, the reservoir of mercury was raised in a manner that would cause some flow of the fresh water out of the model orifices. In order to compensate for the water leg on the manometer tubes connected to the model orifices, the two reference tubes at the ends of the manometer board were connected to a fresh-water reservoir with an open surface 2.6 inches above the free water level of the tank.

Since there were only 100 tubes in the manometer board, only a part of the 246 orifices in the model could be connected on any one run. The orifices connected to the manometer were selected so as to cover the wetted area during the run.

The vertical manometer board was placed about 8 feet from the model and the pressures were recorded with a camera. A second camera was located at the bottom of the towing tank to take underwater photographs as the model passed over it at test speed. The two cameras were operated simultaneously by means of a photoelectric relay arrangement. Typical photographs taken by the two cameras are shown in figures 4 and 5.

The hydrodynamic pressure at a particular orifice in pounds per square inch was obtained as follows. The height of the mercury column corresponding to that orifice was subtracted from the height of the mercury column in the reference tubes; and this difference was multiplied by the difference between the specific weights of mercury and fresh water, 0.453 pound per cubic inch. To this product was added algebraically the correction for the height of the reference-tube water reservoir level above the free water level of the tank (0.094 pound per square inch). The measured pressures, therefore, did not include the static pressures due to the draft of the orifices.

Wetted lengths were obtained from the underwater photographs and were measured from the aft end of the model to the intersection of the heavy spray line with the lower profile as shown on figure 4. Trim was measured as the angle between the center line of the model and the horizontal.

RESULTS AND DISCUSSION

The data are presented in figure 6 for the schedule of test conditions given earlier in the report. Hydrodynamic pressure p in pounds per square inch is plotted against the distance λ in inches measured from the aft end of the model along its center line. Longitudinal distributions are given for each row of orifices located respectively in planes passing through the center line at angles of 0°, 15°, 30°, 45°, and 60° from the lower profile line.

Representative curves indicating effects of change in speed, trim, wetted length, and chine strips are given in figures 7, 8, 9, and 10, respectively. Longitudinal pressure distributions are given in part (a) of these figures and transverse distributions in parts (b) and (c). In figure 7 where the pressures at different speeds are compared, the pressure data are presented as the ratio p/q, but, in the other figures, the pressure p is plotted.

The form of the pressure distributions was similar for all conditions investigated. In the longitudinal direction moving aft, the pressure rose to a positive peak at the stagnation line, then decreased, usually to a negative value, and finally increased to a small value, usually positive. (See, for example, fig. 6(b)). In a transverse direction, from the lower profile line, the positive pressures generally decreased at first and then increased to a peak just inboard of the chine strips. (See, for example, fig. 8(b)). The negative pressure also decreased outboard from the lower profile line but there was no peaking of the negative pressure near the chine strip. (See, for example, fig. 7(c)). It is probable that there is a discontinuity in the transverse pressure distribution across the chine strip. For that reason the faired curve was stopped at the chine strip and the value for $\theta = 60^\circ$ was indicated by a point.

The maximum negative pressures measured were of the order of 0.25 pound per square inch. The magnitude of the maximum negative pressures was the same at 30 feet per second (fig. 6(a)) and at 50 feet per second (fig. 6(b)) but decreased to about zero at 65 feet per second (fig. 6(c)). This effect was most apparent near the lower profile line.

The curves of figure 7 show variation in p/q with speed for a trim of 4° and a wetted-length ratio of about 0.58. The values of p/q at 50 and 65 feet per second are of the same order of magnitude and generally are greater than the values at 30 feet per second. This may indicate that the conditions at 50 and 65 feet per second are closer to pure planing than the condition at 30 feet per second.

The curves of figure 8 show the effect of increase in trim on the pressures obtained. For a given wetted-length ratio and speed, an increase in trim from 4° to 8° resulted in a considerable increase in positive pressure in the vicinity of the stagnation line. However, this increase in trim appeared to have very little effect on the pressures acting on the aft three-quarters of the wetted length. This effect of trim may be attributed, at least partly, to the longitudinal curvature of the streamline body and the manner in which trim has been defined. Thus, the trim of the aft half of the lower profile is less than the center-line trim whereas that of the forward half is greater. Therefore, with increase in center-line trim from 4° to 8°, the trim of the aft three-quarters of the wetted profile still remained fairly small but the trim of the forward quarter increased in a region of comparatively larger trims.

In figure 9 an increase in wetted-length ratio resulted in a large increase in maximum positive pressure and a general movement of the pressure-distribution curve in a positive direction so that the maximum negative pressures were decreased. This effect of increase in wetted length also may be attributed to the longitudinal curvature of the streamline fuselage. In the region of added wetted length, the profile and buttock lines are sweeping upward as wetted length increases, and this apparently results in an increase in effective trim.

The primary effect of the chine strips indicated in figure 10 is a large increase in maximum positive pressure in the region just inboard of the chine strips. The transverse curvature apparently causes a great loss in positive pressure in a transverse direction just aft of the stagnation line unless a discontinuity such as a chine strip is introduced.

CONCLUDING REMARKS

The results from this investigation indicate that there is a characteristic pattern of hydrodynamic pressure distribution for streamline bodies equipped with chine strips and moving on a water surface. In a longitudinal direction moving aft, the pressure rises to a positive peak at the stagnation line, then decreases usually to a negative value and finally increases to a small positive value. In a transverse direction from the lower profile line, the positive pressures generally decreased at first and then increased to a peak just inboard of the chine strips. Negative pressures generally decreased transversely from the profile line without a pronounced peak at the chine strip. The maximum negative pressure measured was about 0.25 pound per square inch.

Langley Aeronautical Laboratory,
National Advisory Committee for Aeronautics,
Langley Field, Va., June 9, 1955.

REFERENCES

1. Weinflash, Bernard, and Fontana, Rudolph E.: The Hydrodynamic Force Characteristics of Streamline Bodies of Revolution Having Fineness Ratios of 6, 9, and 12 With and Without Chine Strips. NACA RM L54K22, 1955.

2. Rayle, Roy E., Jr.: An Investigation of the Influence of Orifice Geometry on Static Pressure Measurements. M. S. Thesis, M. I. T., 1949.

3. Kapryan, Walter J., and Boyd, George M., Jr.: Hydrodynamic Pressure Distributions Obtained During a Planing Investigation of Five Related Prismatic Surfaces. NACA TN 3477, 1955.

TABLE I

MODEL OFFSETS

Station, x, in.	Diameter, d, in.
0	0
.47	1.11
.98	1.50
1.96	2.09
2.90	2.51
3.88	2.87
5.84	3.44
7.81	3.88
9.72	4.22
11.69	4.49
15.57	4.90
19.49	5.12
23.38	5.20
27.26	5.04
31.18	4.59
35.06	3.81
38.94	2.67
40.91	2.04
42.87	1.38
44.79	.70
45.76	.35
46.75	0

TABLE II

LOCATION OF ORIFICES

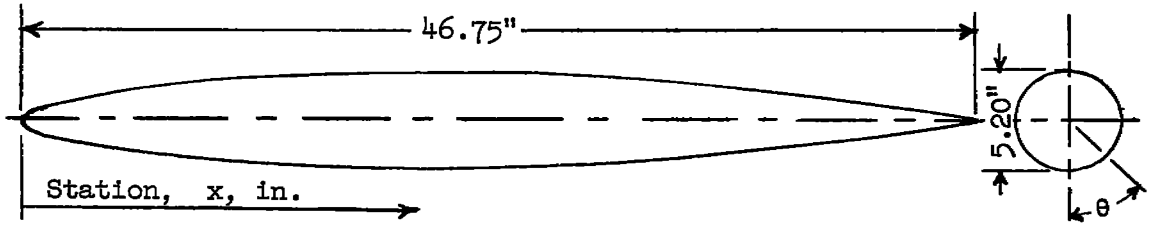

Station, x, in.	Region covered by orifices				
	θ = 0°	θ = 15°	θ = 30°	θ = 45°	θ = 60°
1	—			—	—
2					
3					
4					
5					
6					
$6\frac{1}{2}$					
7			—		
$7\frac{1}{2}$		—			
8					
$8\frac{1}{2}$					
9 to 30[a]					
$30\frac{1}{2}$ to $35\frac{1}{2}$[b]					
36					
37					
38					
39					
40		—	—		
41					
42					
43					
44					
45				—	—
46	—				

[a]1-inch longitudinal spacing.

[b]1/2-inch longitudinal spacing.

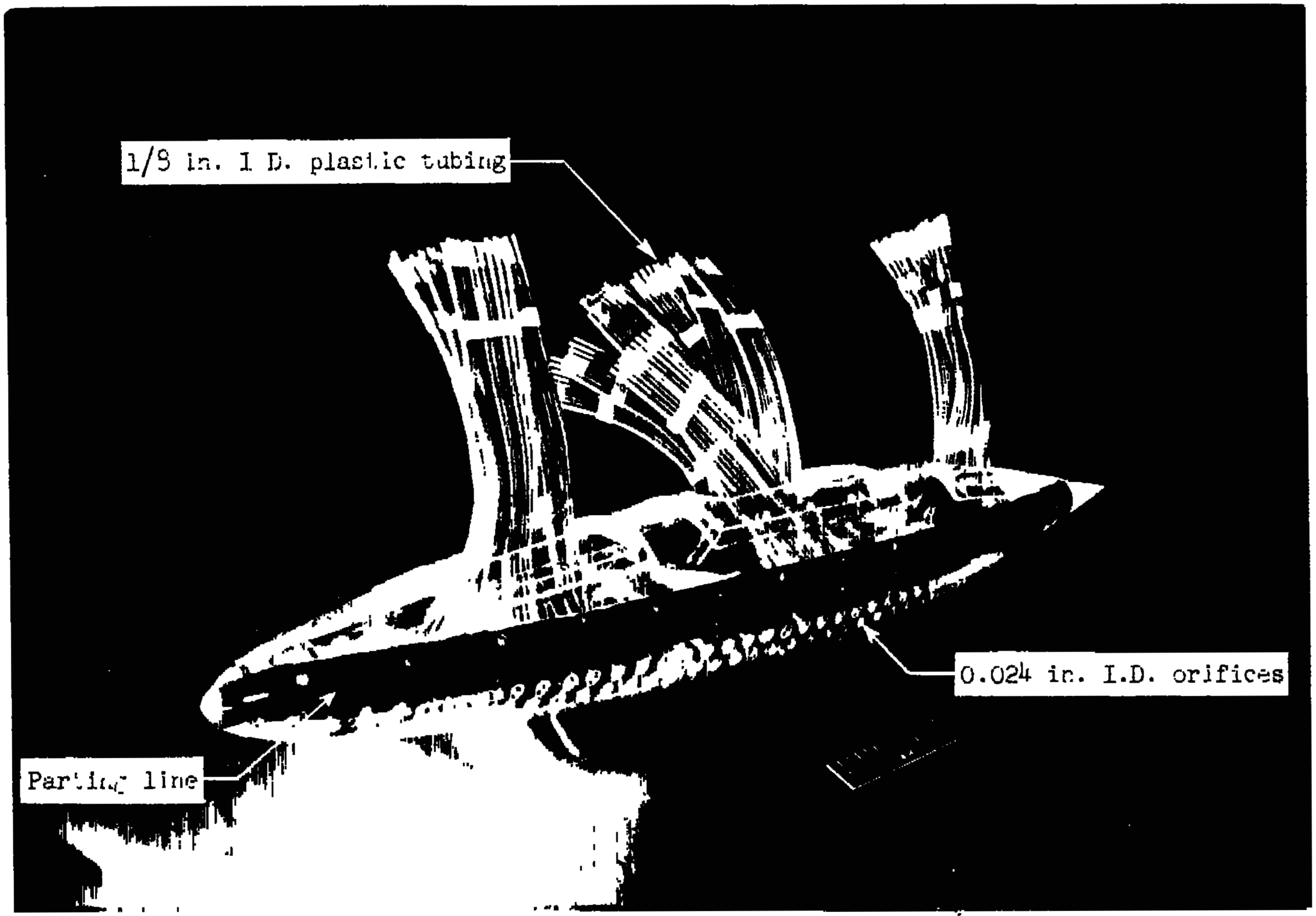

L-77679.1

Figure 1.- Photograph of model.

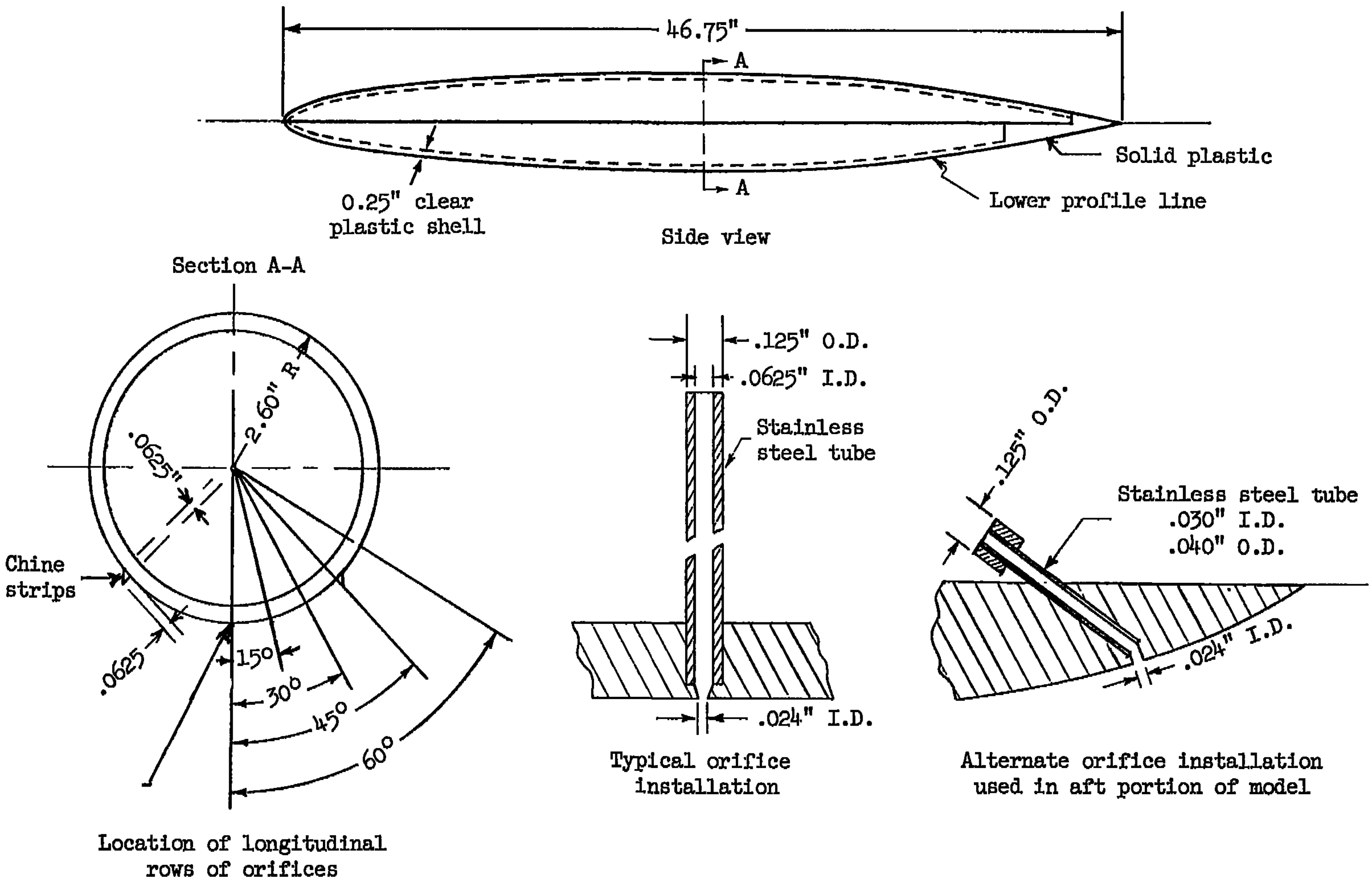

Figure 2.- Model details.

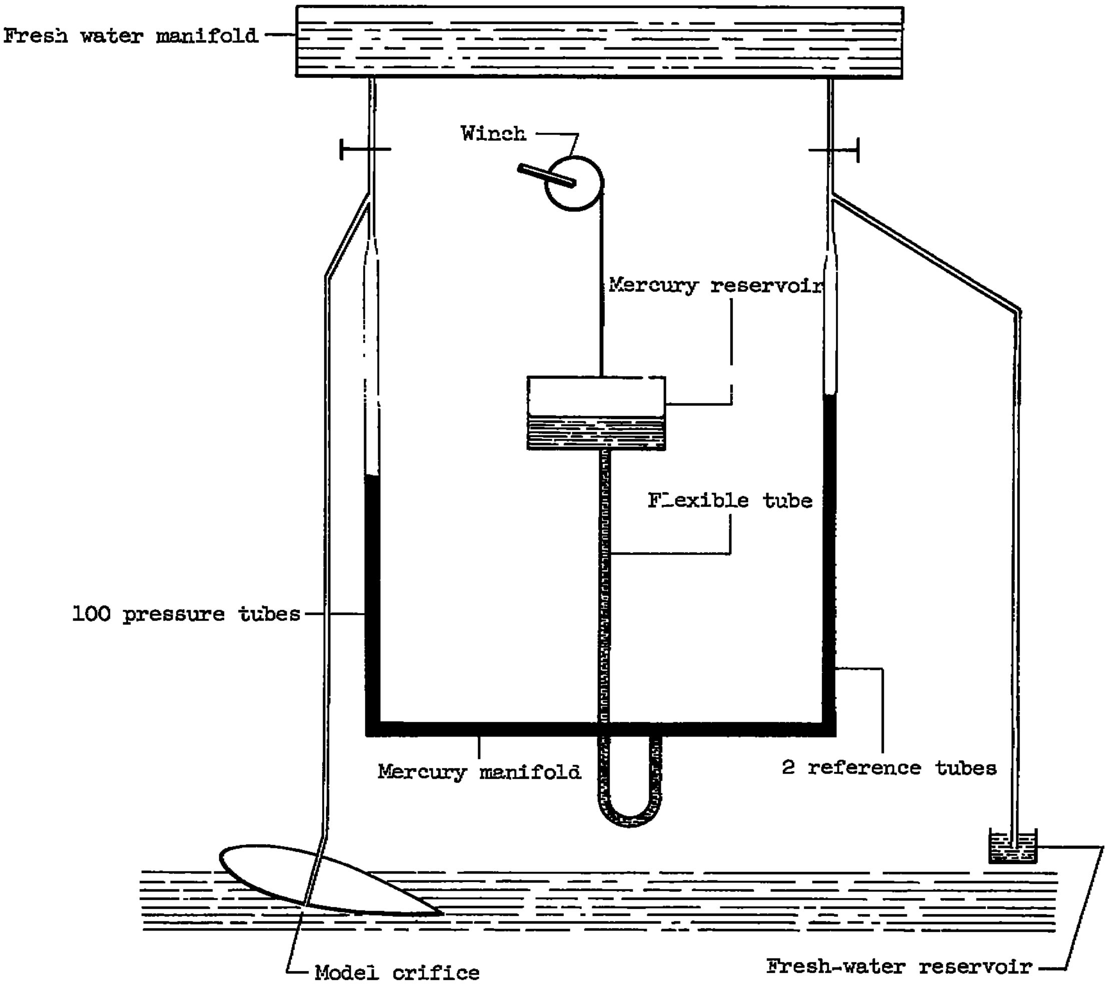

Figure 3.- Schematic illustration of method of measuring pressures.

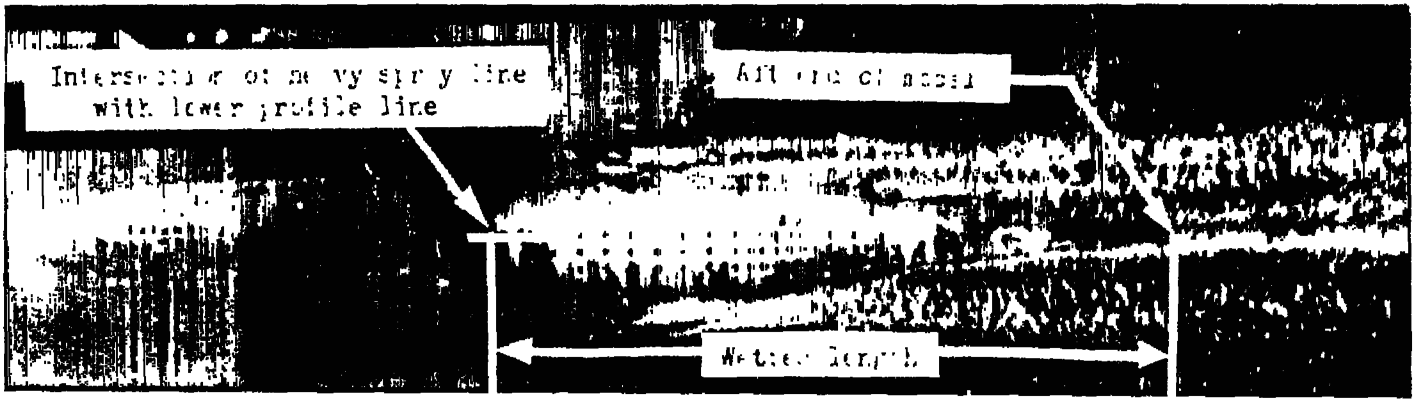

L-89349

Figure 4.- Underwater photograph illustrating method of obtaining wetted length.

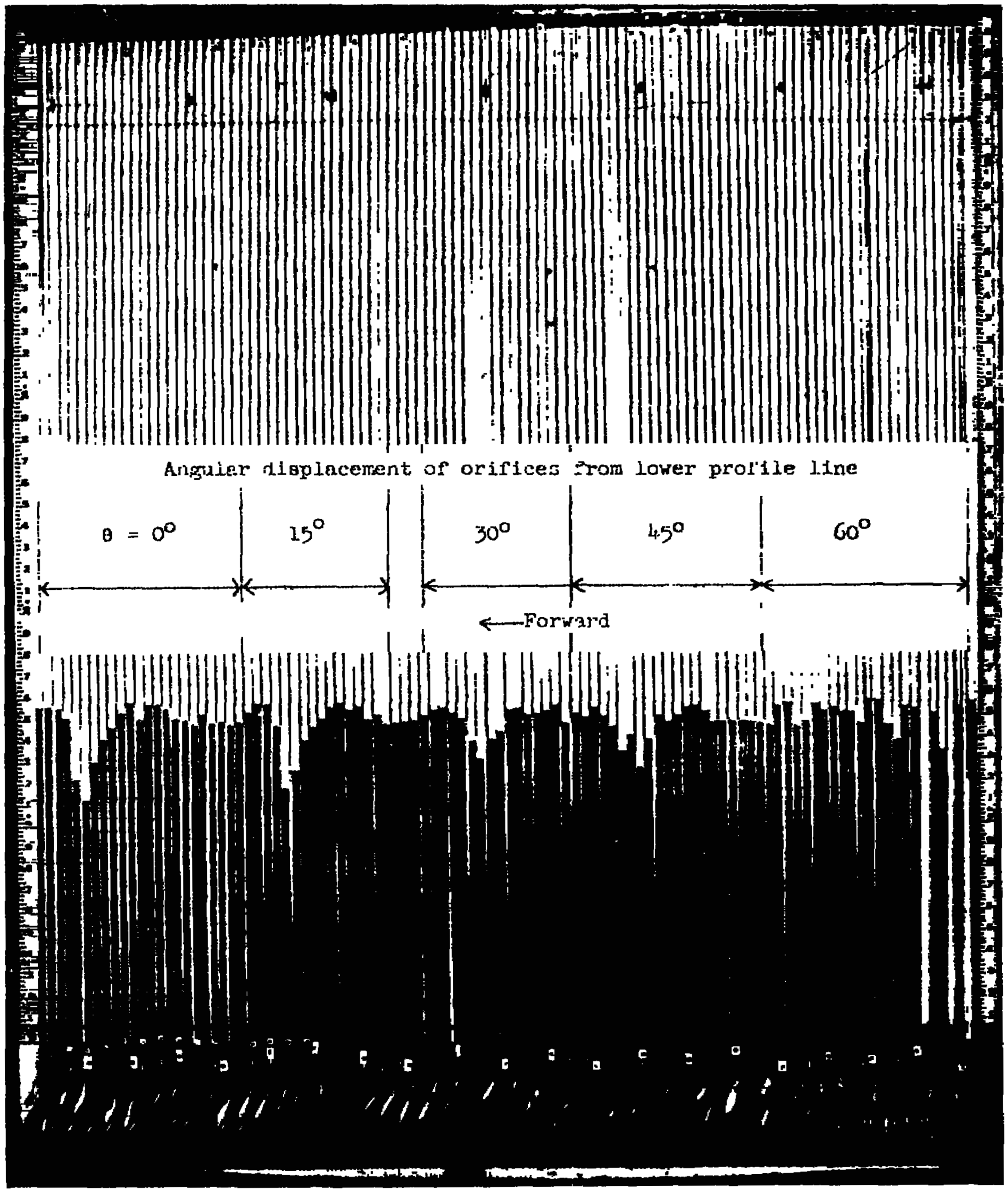

L-89373

Figure 5.- Typical test record (run 3).

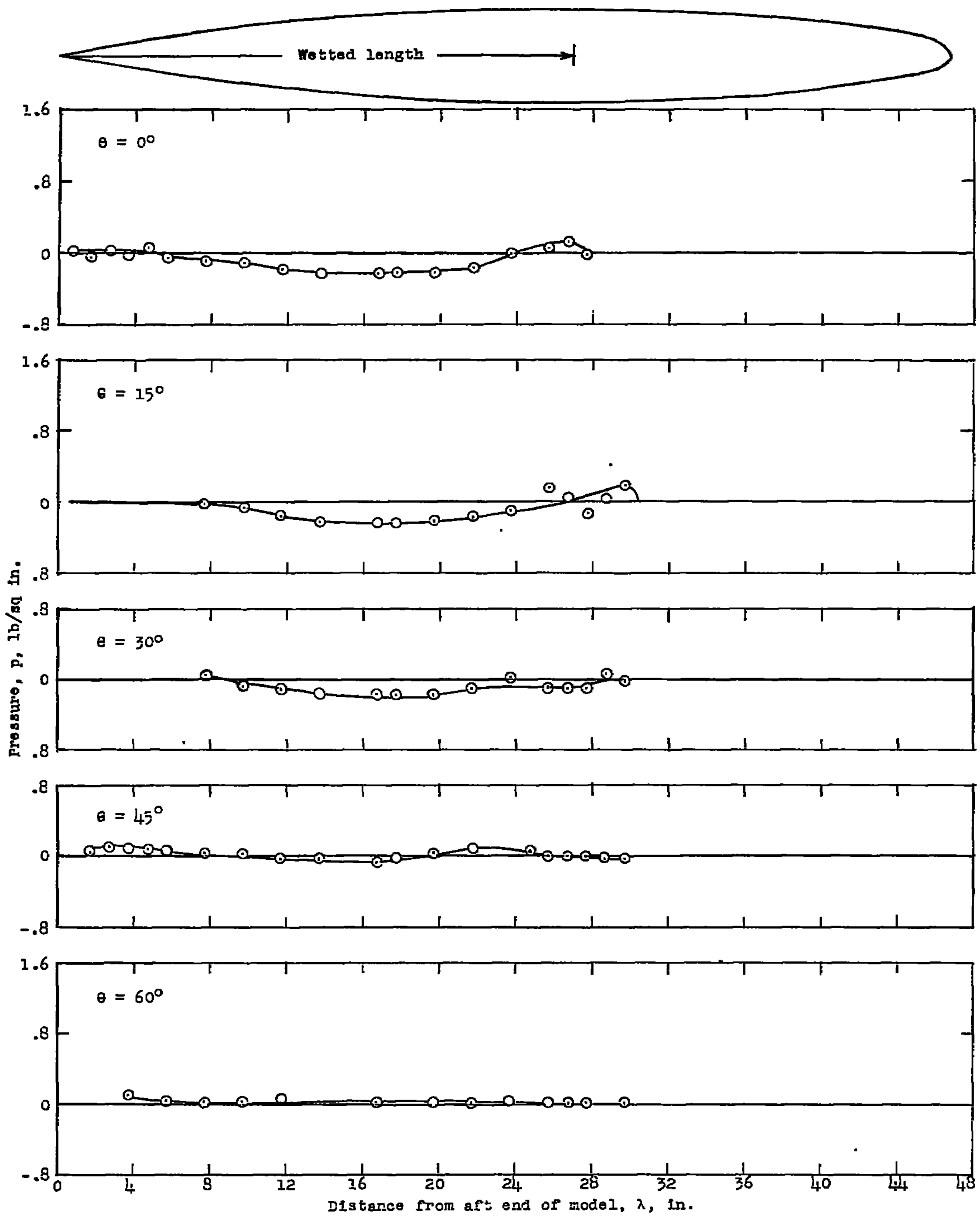

(a) V = 30 feet per second; τ = 4°; l/L = 0.58; strips on; run 1.

Figure 6.- Pressure data.

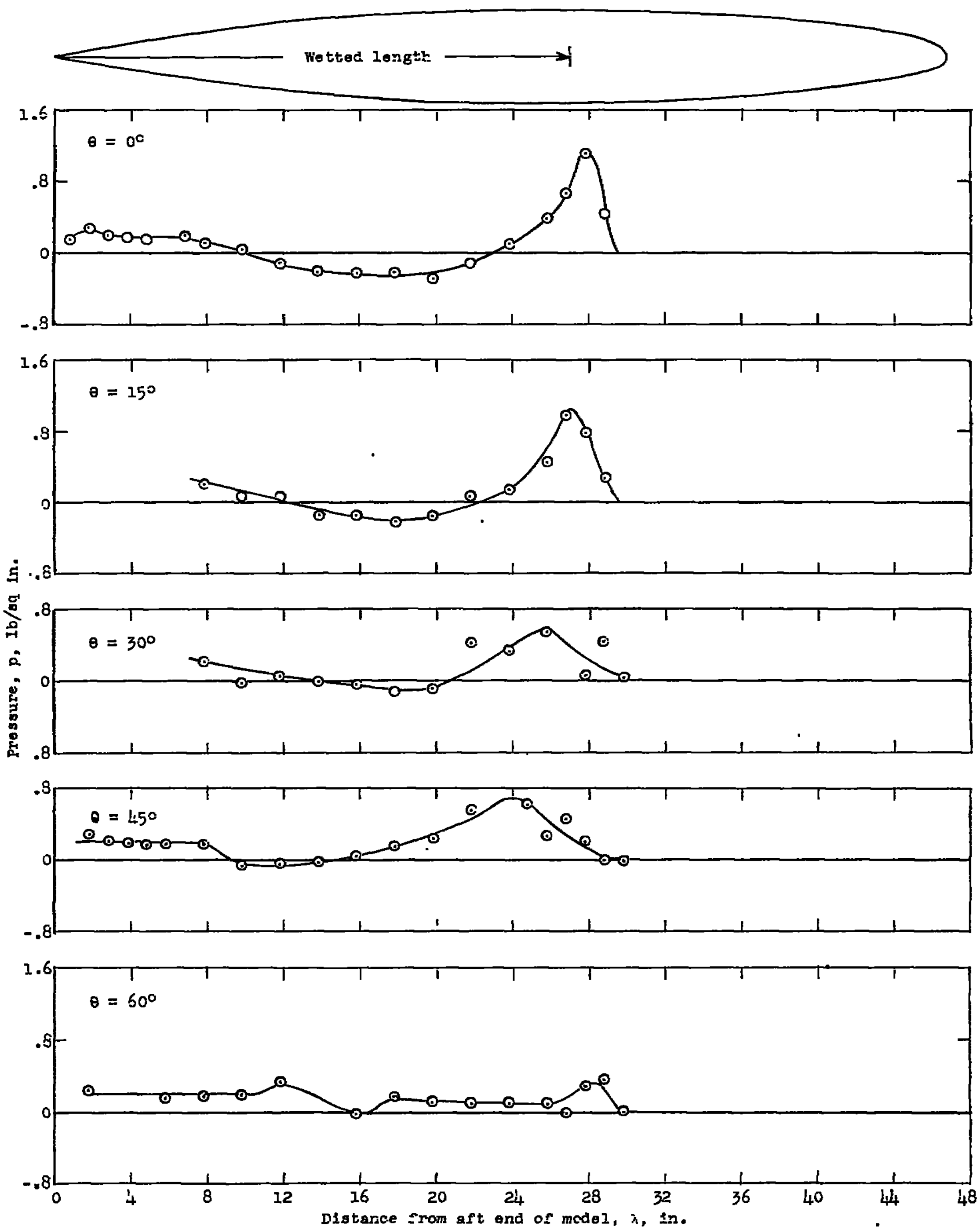

(b) $V = 50$ feet per second; $\tau = 4^{\circ}$; $l/L = 0.58$; strips on; run 2.

Figure 6.- Continued.

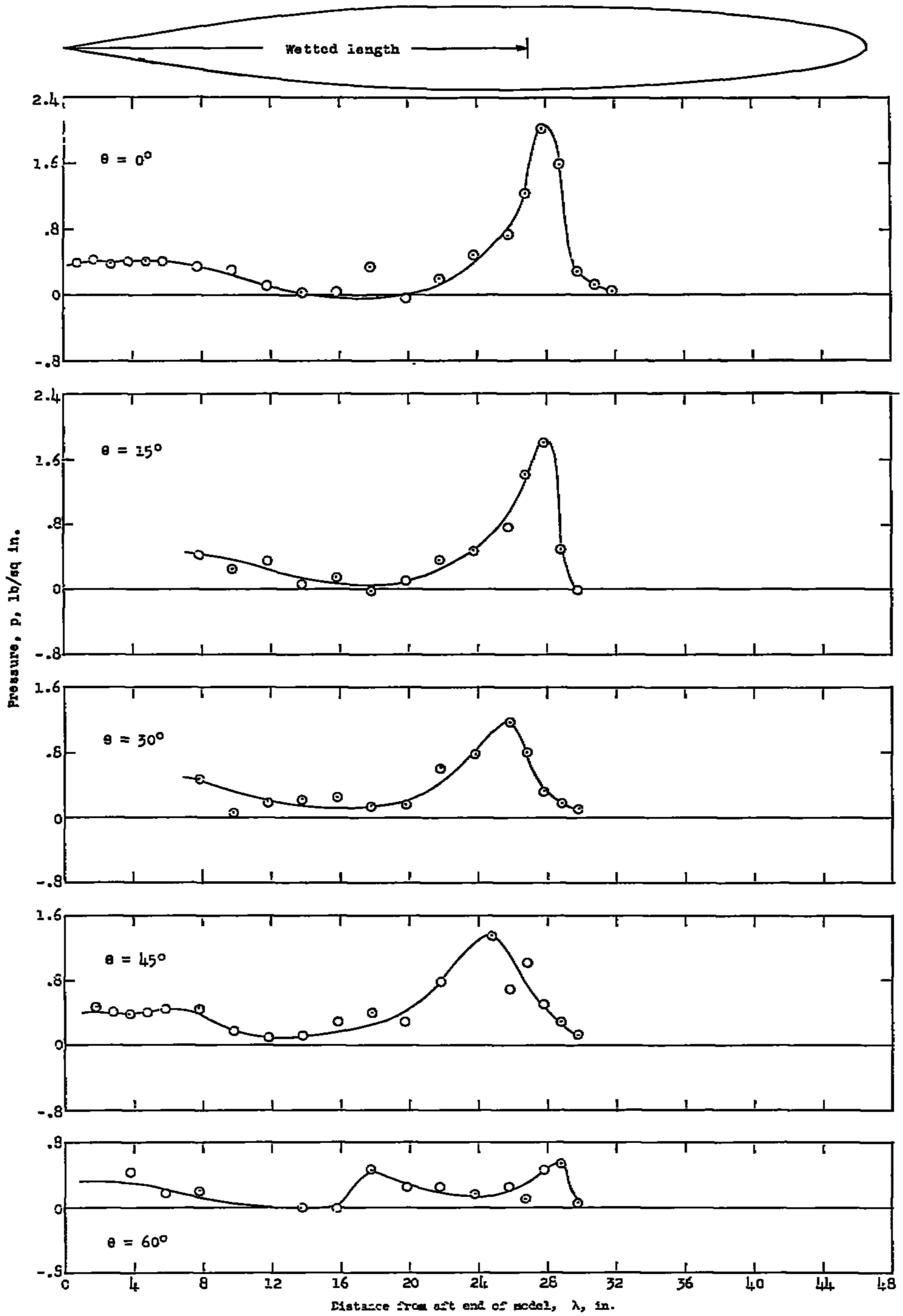

(c) V = 65 feet per second; $\tau = 4^{\circ}$; $l/L = 0.58$; strips on; run 3.

Figure 6.- Continued.

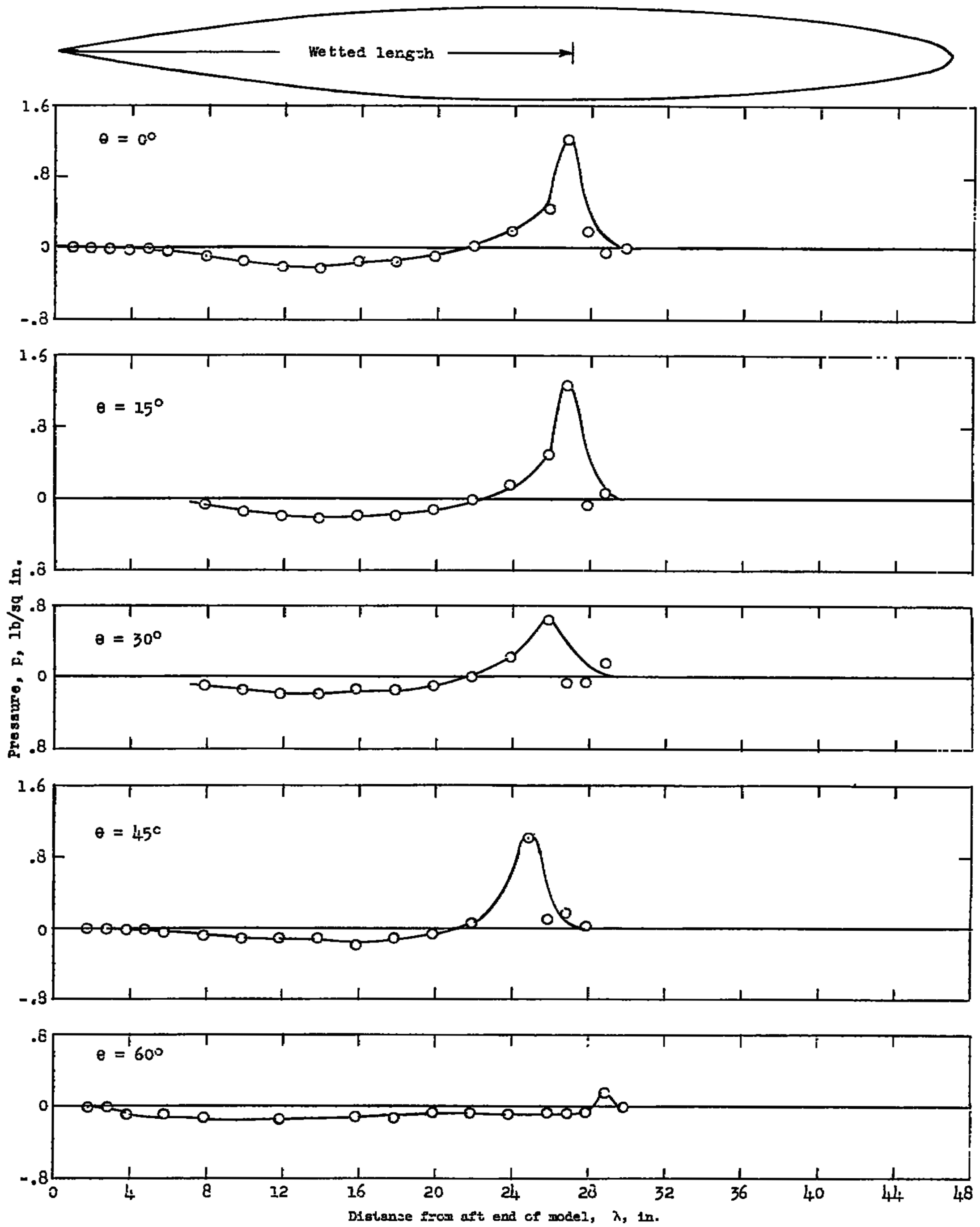

(d) V = 30 feet per second; $\tau = 8^{\circ}$; $l/L = 0.58$; strips on; run 4.

Figure 6.- Continued.

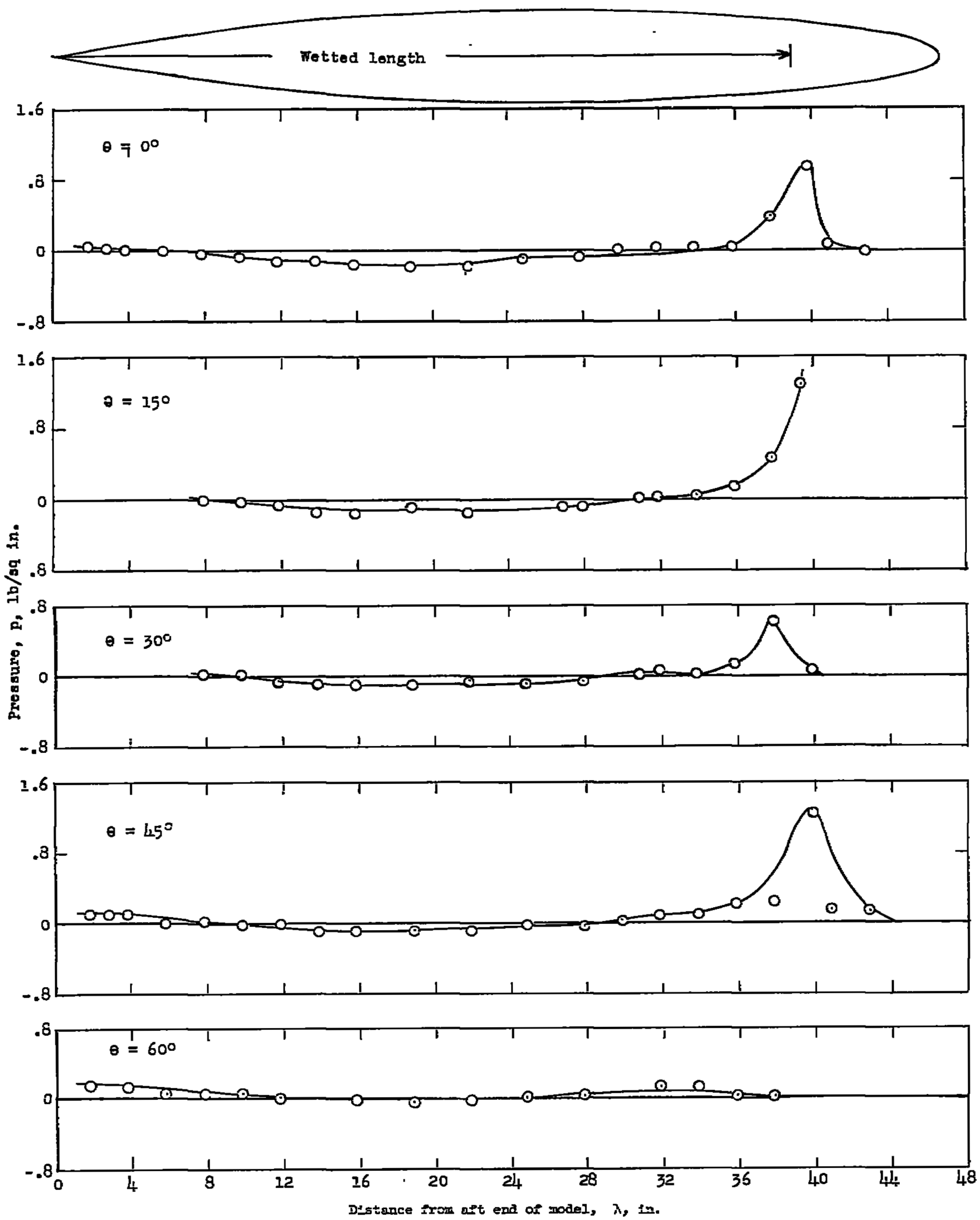

(e) V = 30 feet per second; $\tau = 4^{\circ}$; $l/L = 0.83$; strips on; run 5.

Figure 6.- Continued.

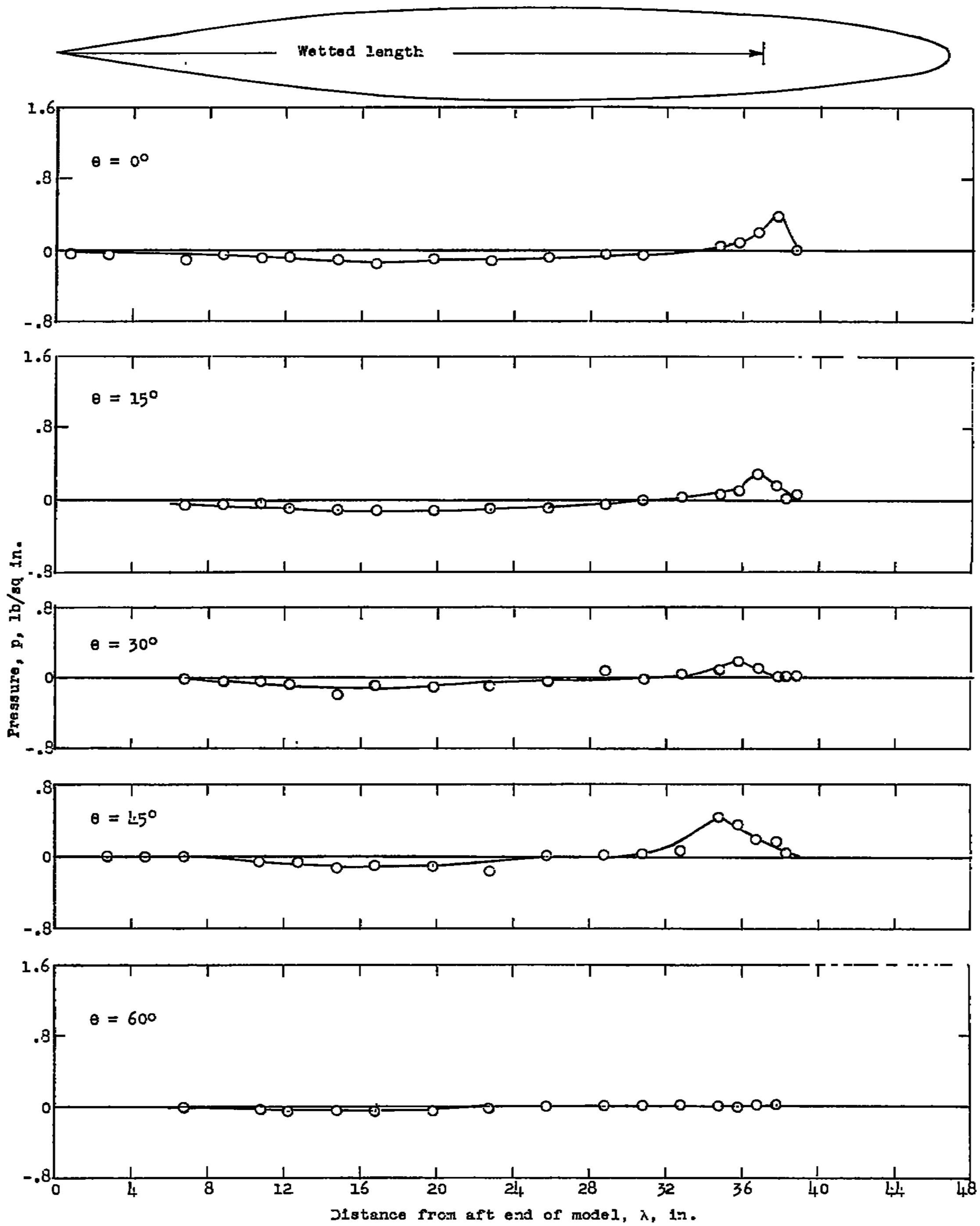

(f) V = 20 feet per second; τ = 4°; l/L = 0.79; strips on; run 6.

Figure 6.- Continued.

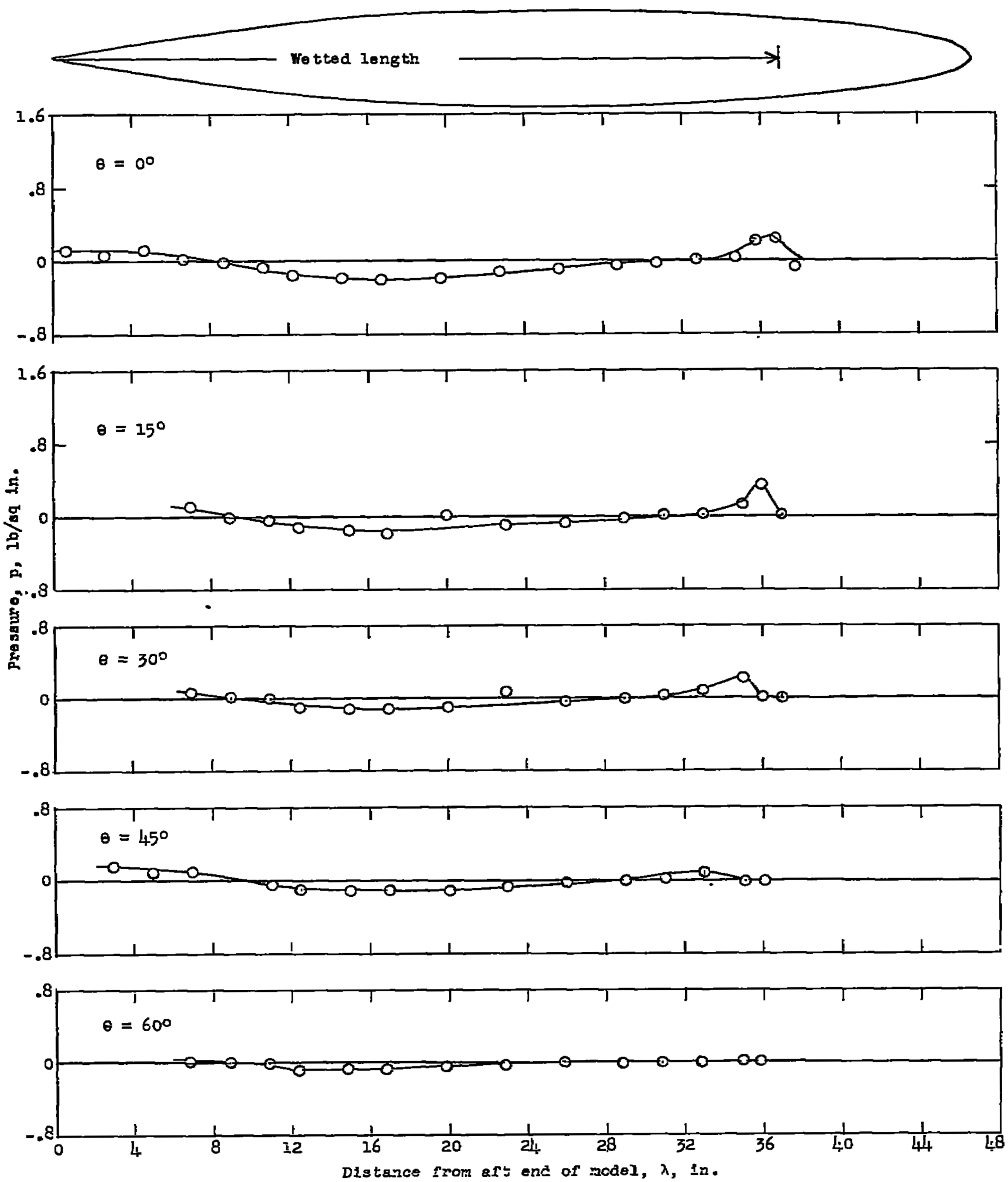

(g) V = 20 feet per second; $\tau = 4^{\circ}$; $l/L = 0.79$; strips off; run 7.

Figure 6.- Concluded.

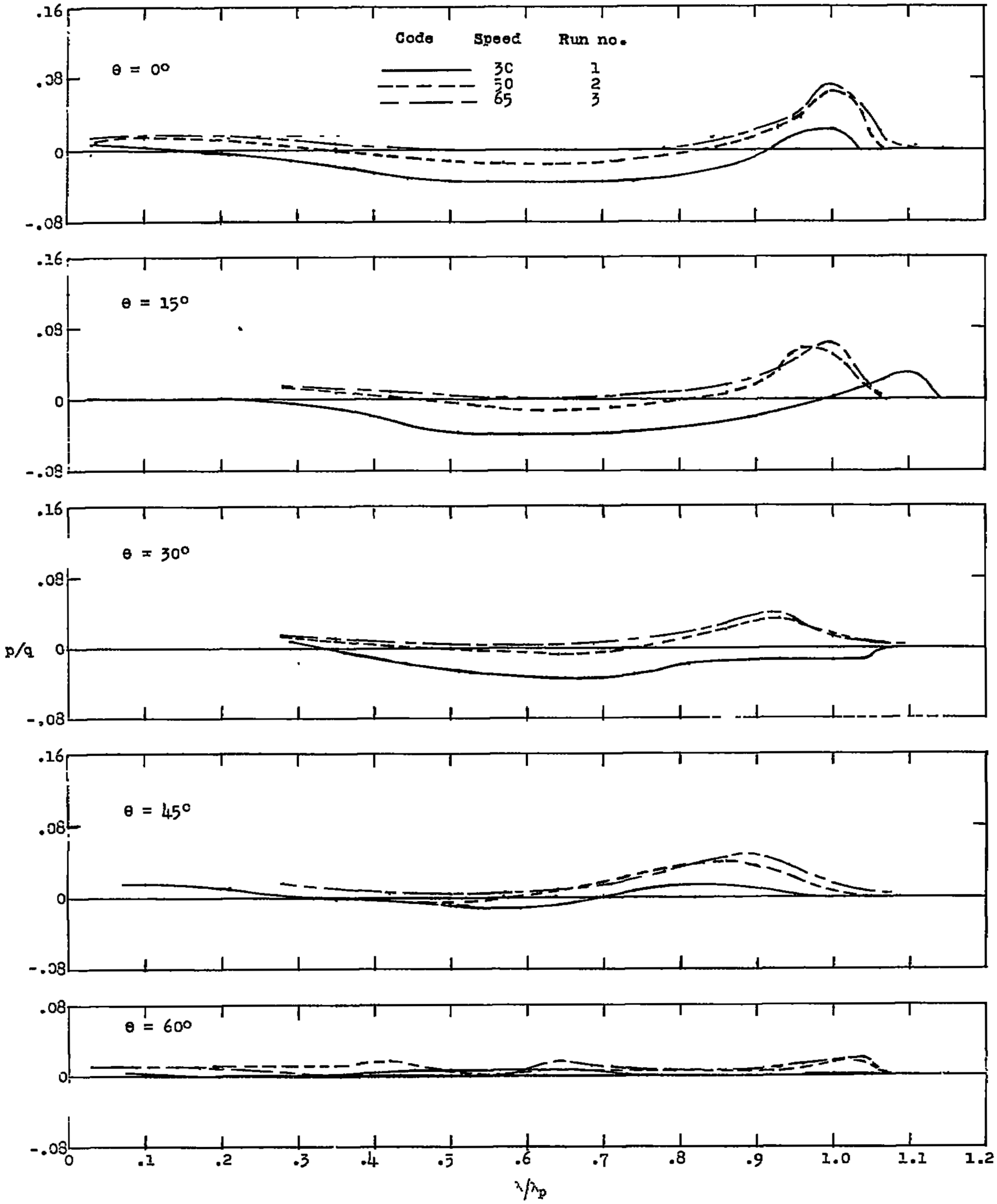

(a) Longitudinal distribution of pressure.

Figure 7.- Effect of speed. $\tau = 4^{\circ}$; $l/L = 0.58$; strips on.

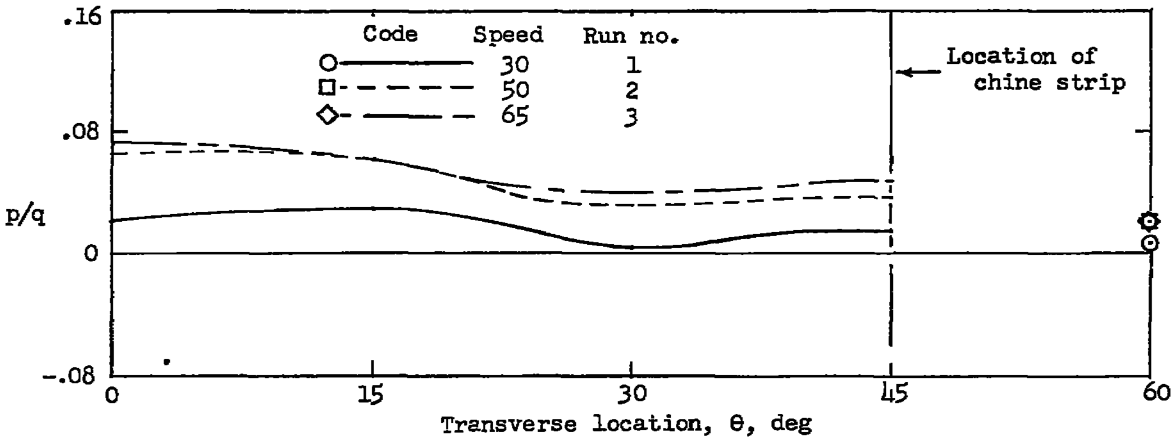

(b) Transverse distribution of peak pressures in vicinity of stagnation line.

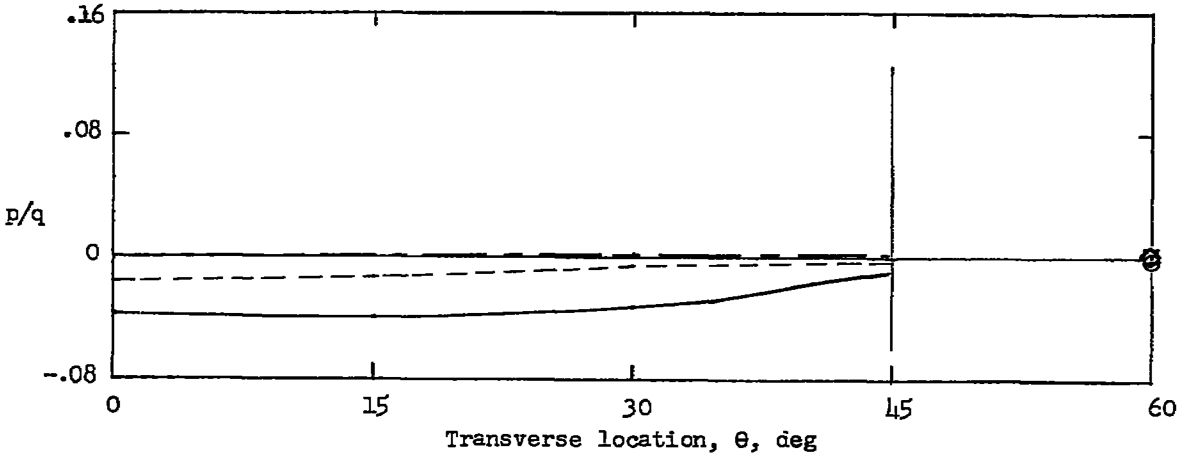

(c) Transverse distribution of largest negative pressures aft of the peak pressures.

Figure 7.- Concluded.

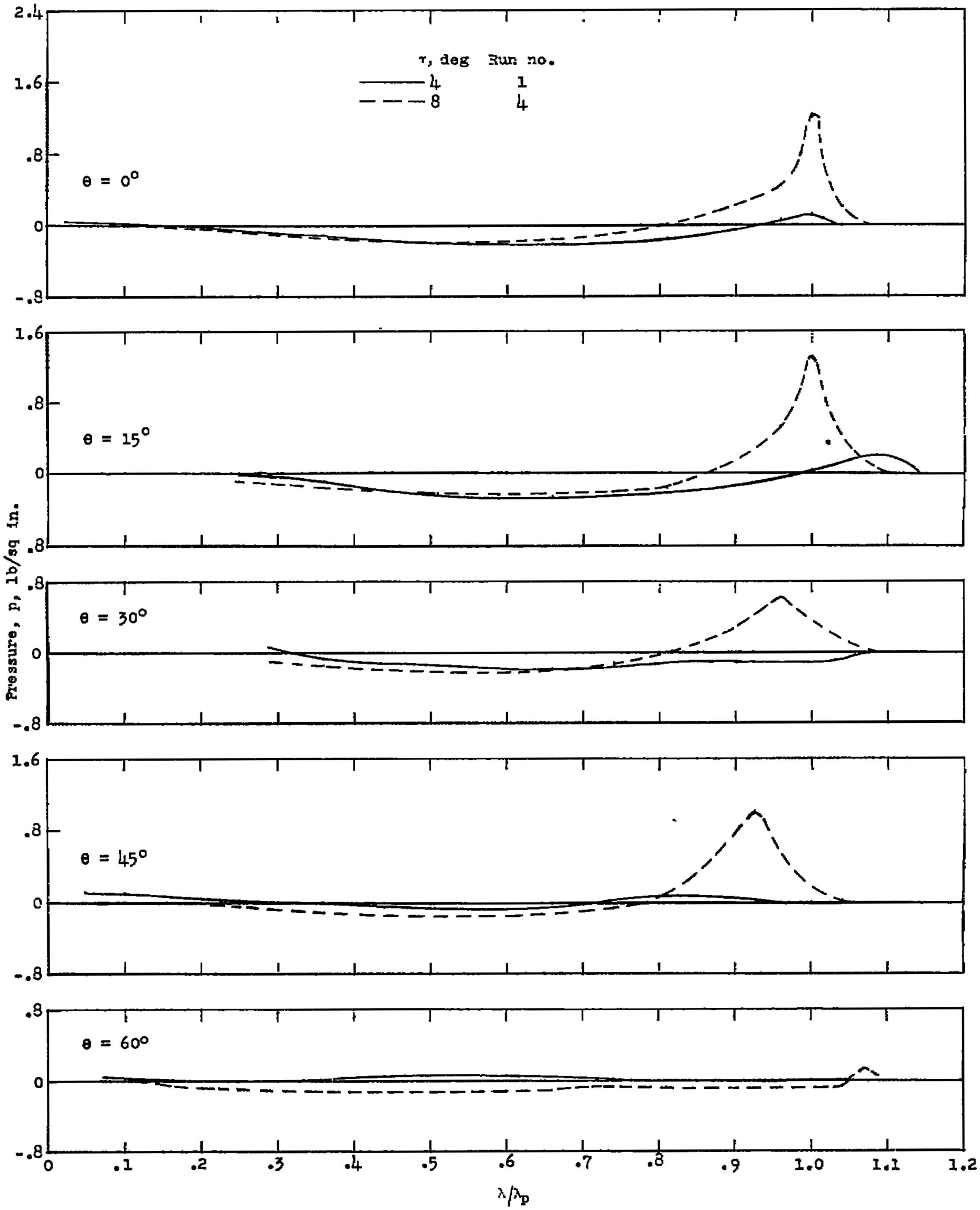

(a) Longitudinal distribution of pressure.

Figure 8.- Effect of trim. V = 30 feet per second; $l/L = 0.58$; strips on.

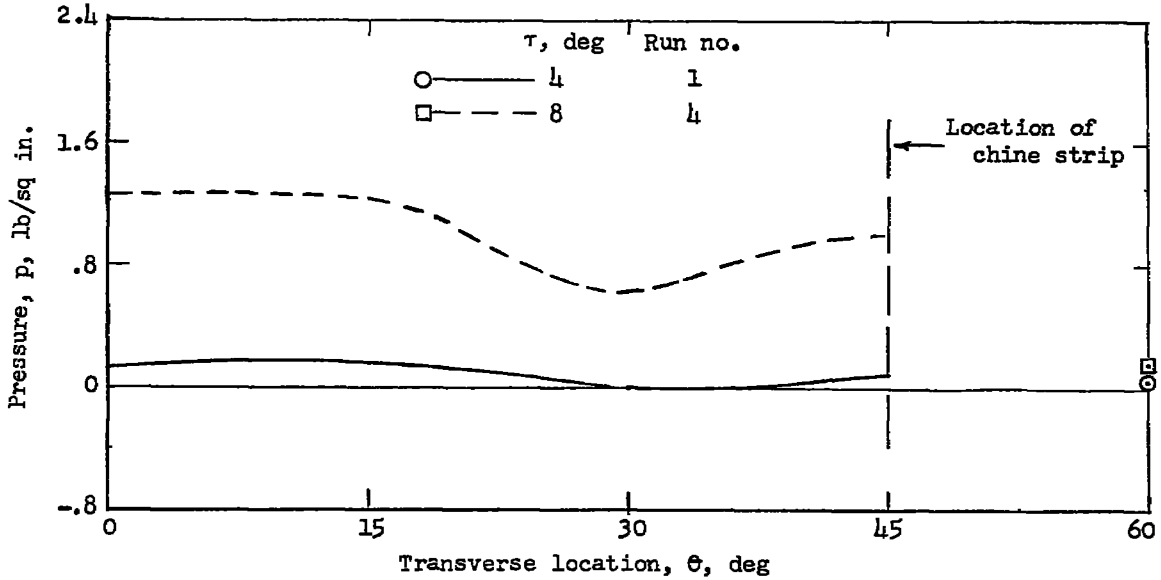

(b) Transverse distribution of peak pressures in vicinity of stagnation line.

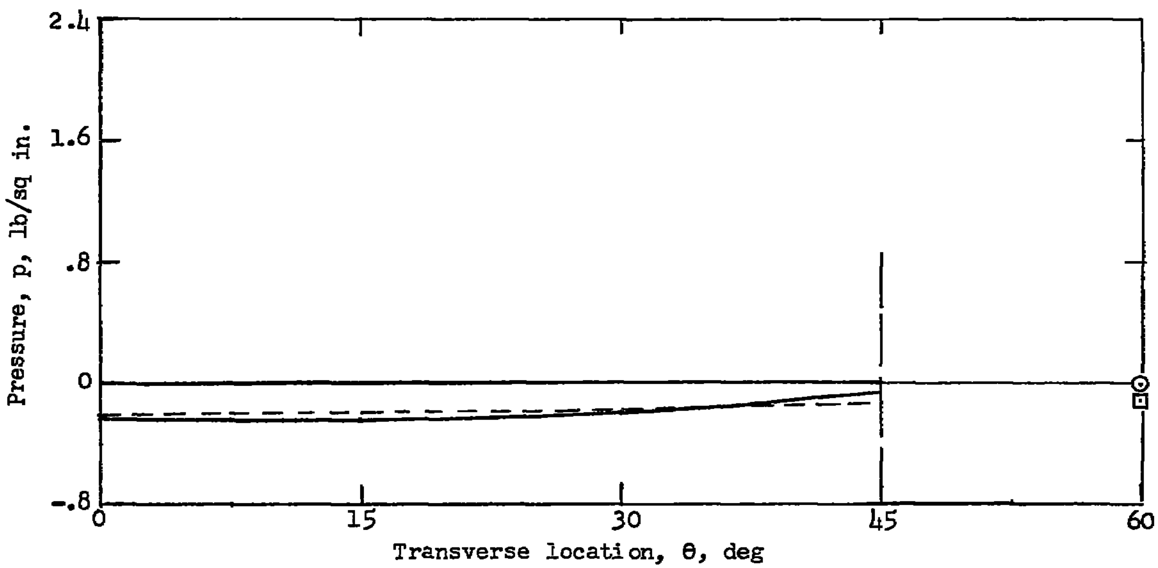

(c) Transverse distribution of largest negative pressures aft of the peak pressures.

Figure 8.- Concluded.

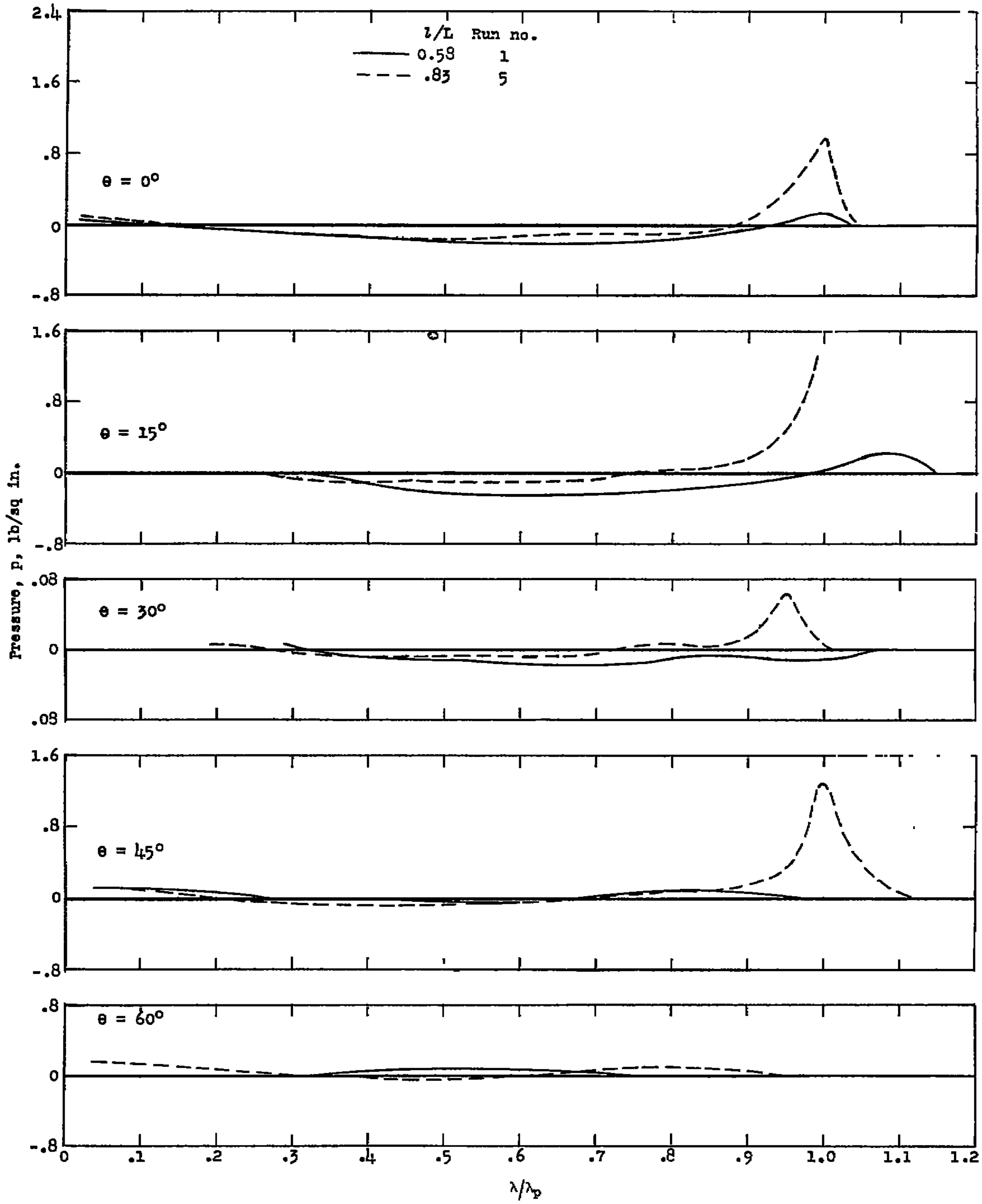

(a) Longitudinal distribution of pressure.

Figure 9.- Effect of wetted length. V = 30 feet per second; $\tau = 4^{\circ}$; strips on.

[redacted]

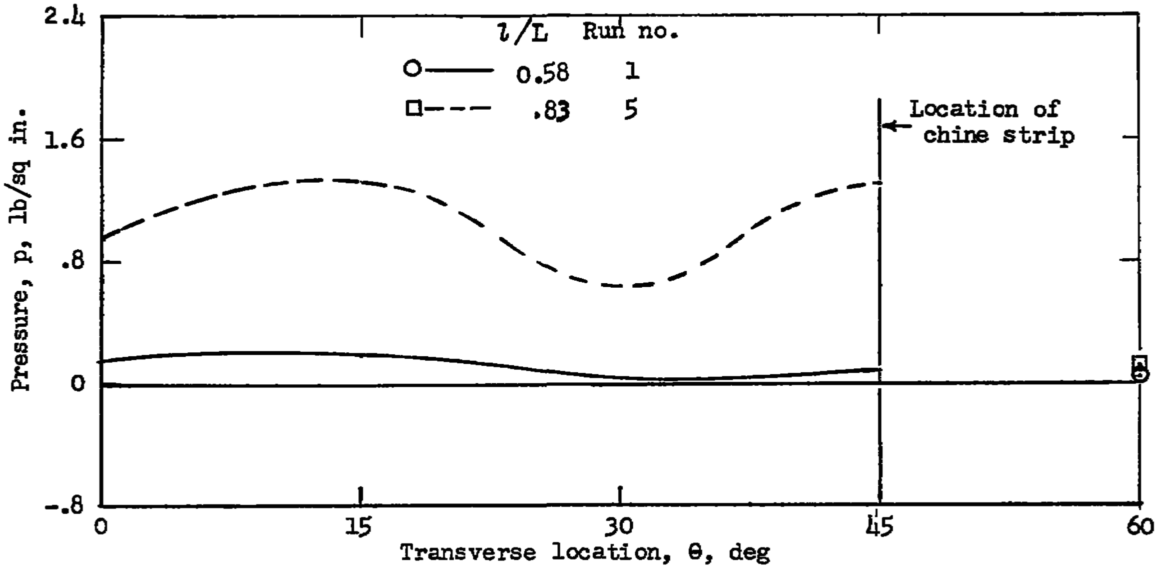

(b) Transverse distribution of peak pressures in vicinity of stagnation line.

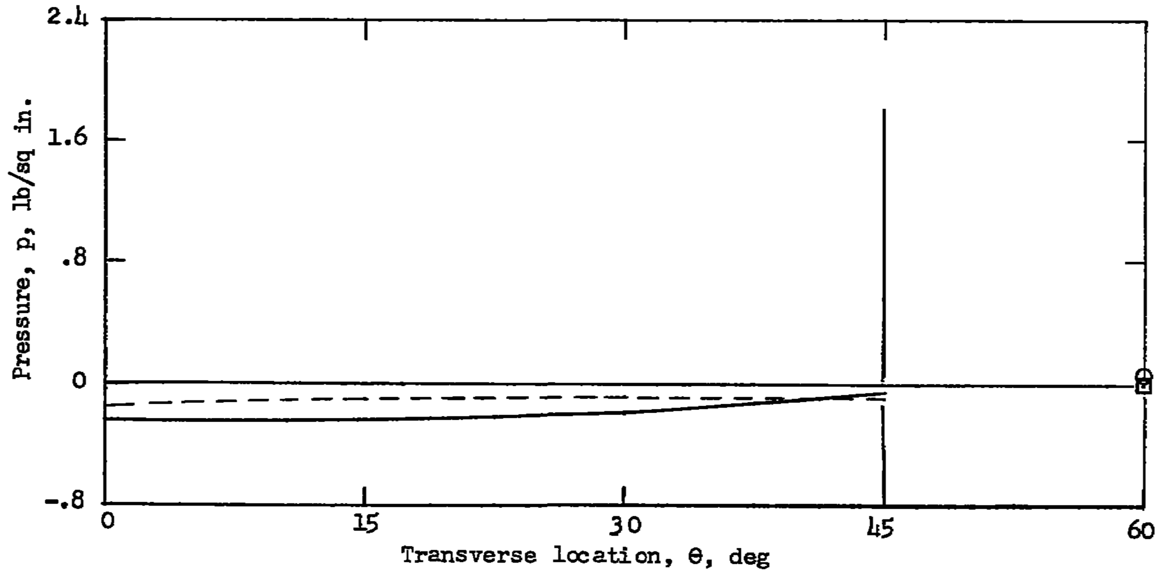

(c) Transverse distribution of largest negative pressures aft of the peak pressures.

Figure 9.- Concluded.

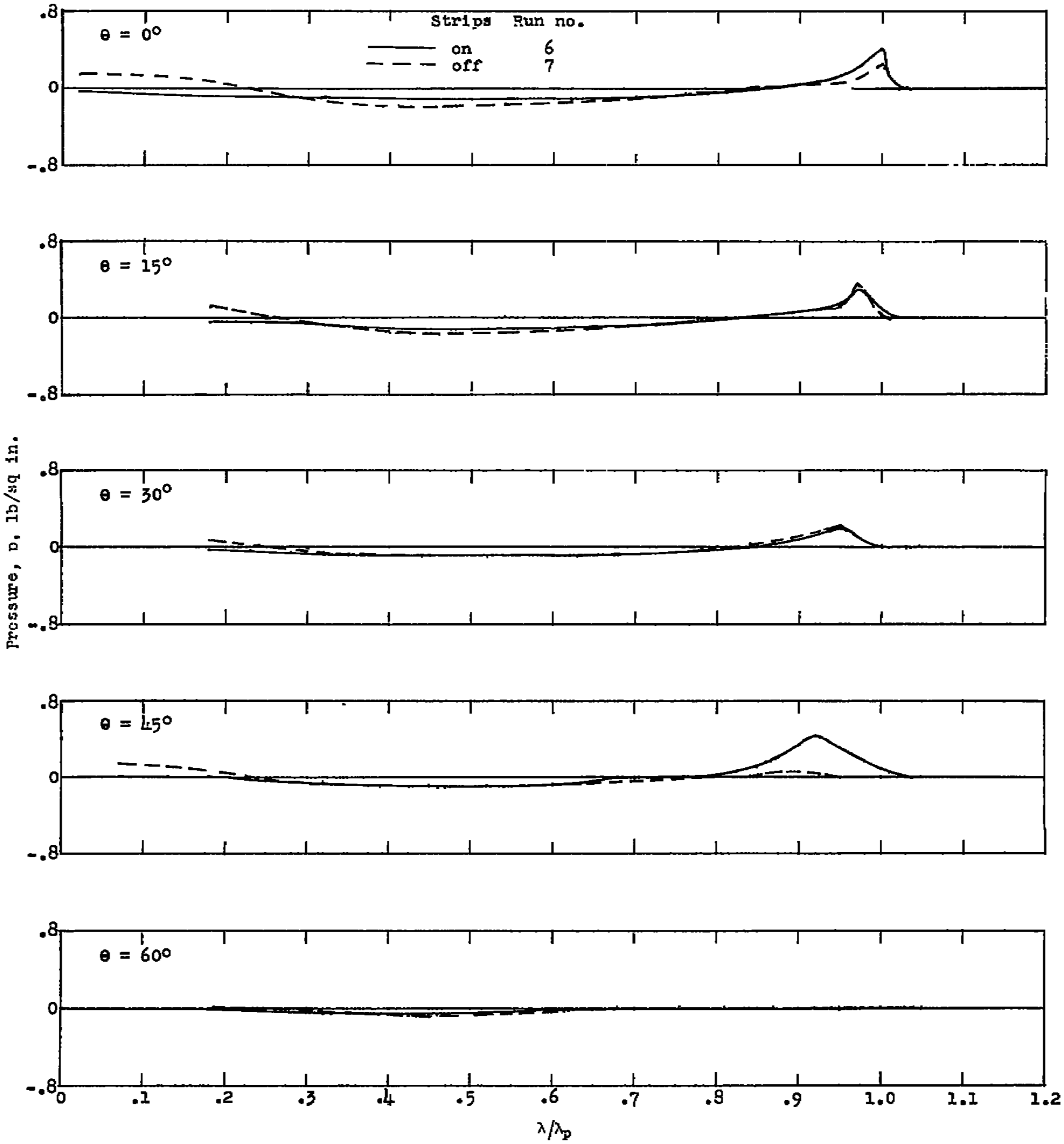

(a) Longitudinal distribution of pressure.

Figure 10.- Effect of chine strips. $V = 20$ feet per second; $\tau = 4^\circ$; $l/L = 0.79$.

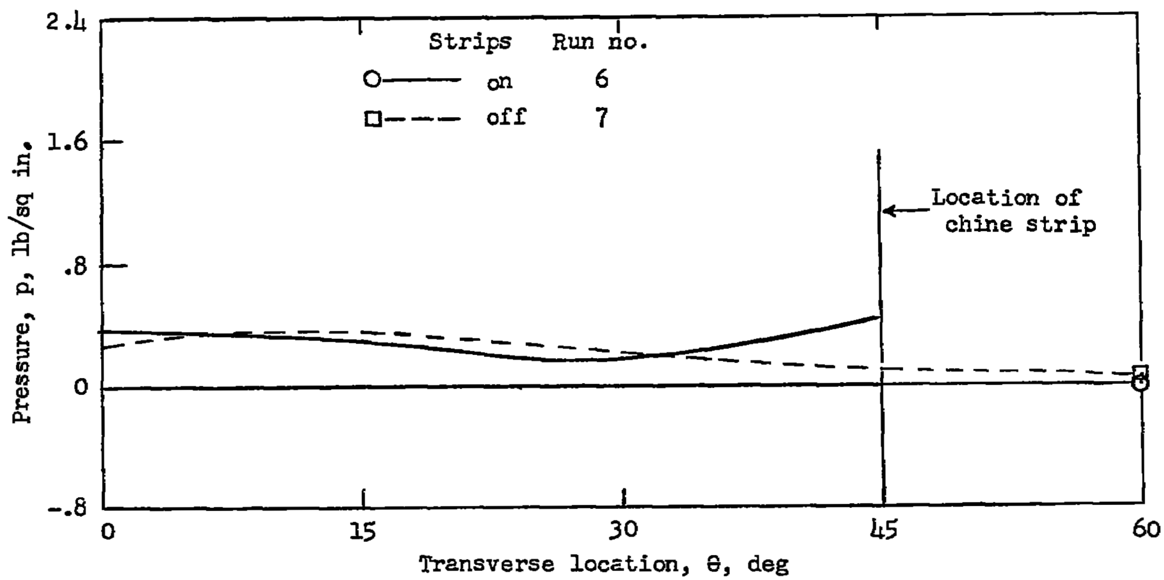

(b) Transverse distribution of peak pressures in vicinity of stagnation line.

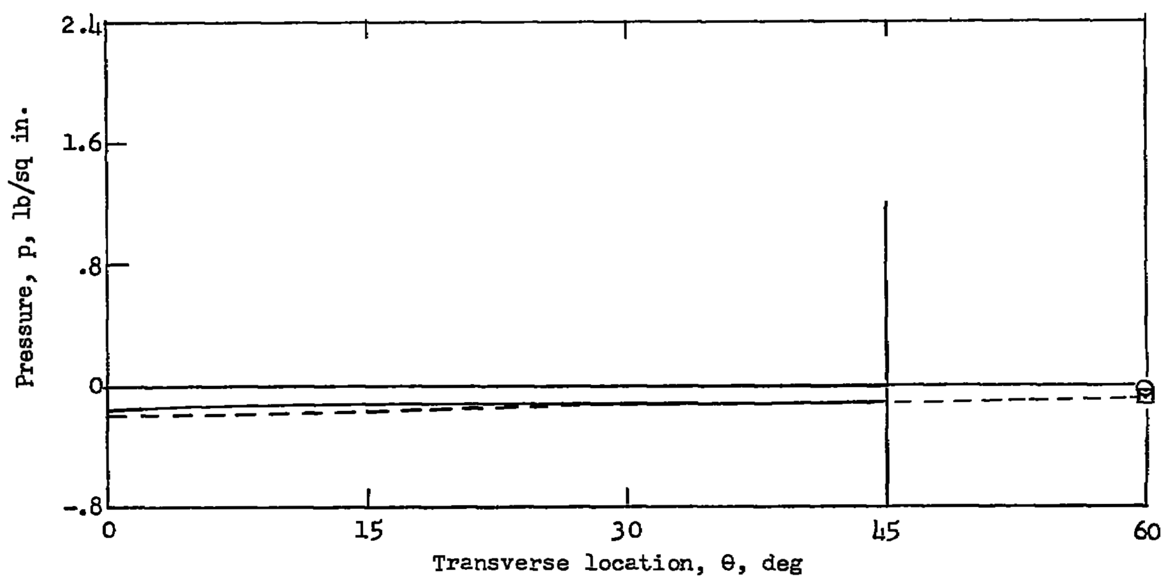

(c) Transverse distribution of largest negative pressures aft of the peak pressures.

Figure 10.- Concluded.

[redacted]